Numerical and Experimental Analysis of Airfoil Profile

Nitesh Kumar Yadav[1], Shailesh KC[1], Ramesh Chand[1], Osan Malla[1], Rijan Bhusal[1], Santosh Lamsal[1], Dipesh Karki[1*]
[1]Department of Mechanical and Automobile Engineering, Pashchimanchal Campus, Institute of Engineering, Tribhuvan University
*dipeshk@wrc.edu.np
(Manuscript Received 20th April, 2025; Revised 14th May, 2025; Accepted 20th May, 2025)

Abstract

This project presents a combined numerical and experimental analysis of the aerodynamic behavior of the NACA 0015 airfoil, focusing on lift characteristics. The experimental investigation was conducted in an open-type subsonic wind tunnel at the Institute of Engineering, Pashchimanchal Campus, with airflow velocities 9–16m/s. Numerical simulations were performed using ANSYS Fluent, applying the standard k-epsilon turbulence model across different inlet velocities. Lift forces obtained from both approaches were compared to evaluating accuracy and consistency. The results showed good agreement between experimental and CFD data, particularly at angles of attack 10° and 15°, validating the effectiveness of CFD as an alternative to experimental methods. This study enhances the understanding of flow behavior around airfoils and provides a foundation for further investigations into performance optimization in aerospace and engineering applications.
Keyword: *CFD, Lift force, Simulation, Validation, Wind Tunnel*

1. Introduction

The study of flow over airfoil profile is fundamental in external aerodynamics (Anderson, 2011). These geometries play a crucial role in a wide range of engineering applications such as aircraft wings, wind turbine blades, and structural components like bridges. Accurate prediction of aerodynamic performance, especially lift and drag forces, under varying Reynolds numbers and angles of attack (AOA), is essential for performance optimization and safety considerations (Rubel et al., 2016).

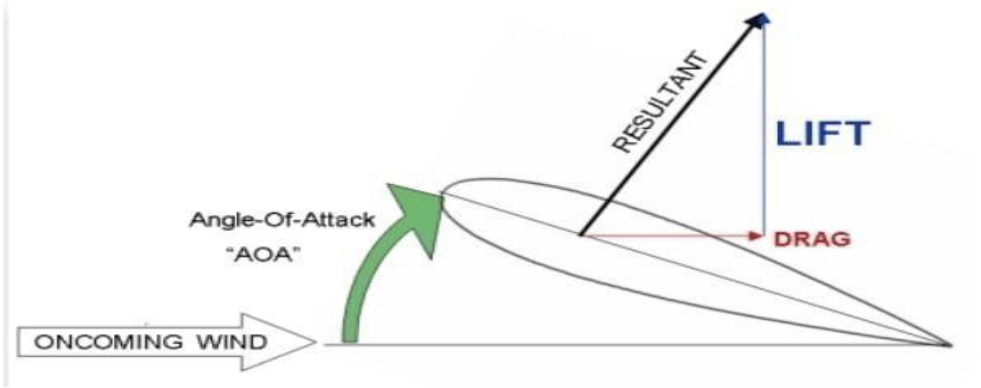

Fig. 1: Lift and Drag on an Airfoil at Angle of Attack (Dreesecode, 2025).

As illustrated in Fig. 1, the lift force acts perpendicular to the relative flow direction, while drag acts in opposition to it. The resultant aerodynamic force is a vector sum of these two. The magnitude of lift and drag is significantly influenced by the angle of attack, surface geometry, and the flow regime (Boyle, 1988).

This study focuses on the NACA 0015 air foil, a symmetric profile (Fig. 2) frequently used in wind turbine blades and control surfaces. Its symmetry makes it a suitable candidate for studying flow separation and stall behavior under both positive and negative angles of attack (Sahin and Acir, February 2015).

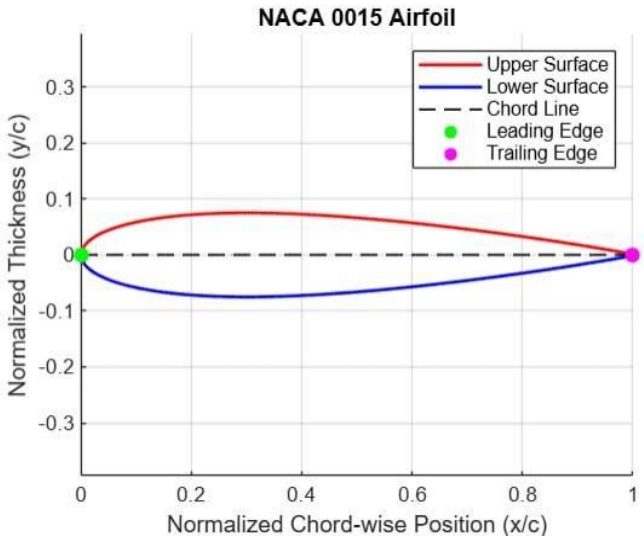

Fig. 2: Airfoil Profile (NACA 0015).

Experimental validation was conducted in a sub sonic wind tunnel facility at IOE Pashchimanchal Campus, as shown in Fig. 3.

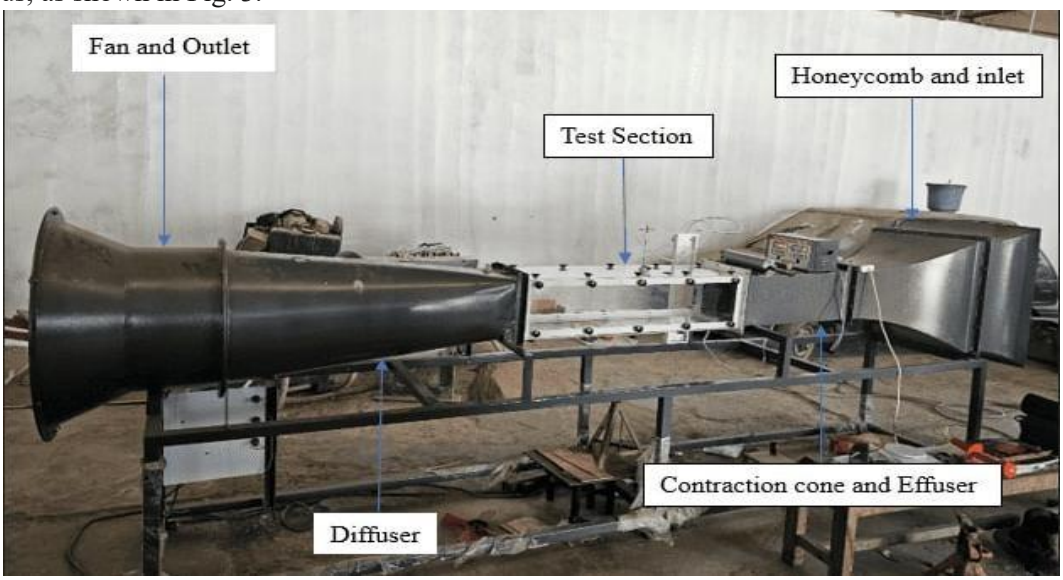

Fig. 3: Wind Tunnel Test Rig at IOE Paschimanchal Campus.

The test rig consists of an inlet honeycomb structure, contraction cone, test section, and diffuser. This controlled environment enables accurate measurement of aerodynamic forces on test objects such as airfoils and cylinders. These measurements are used to validate Computational Fluid Dynamics (CFD) results obtained using the k-epsilon turbulence model (RNG, 2012).

2. Methodology

The k-ε turbulence model is applied for numerical simulations. The analysis involves structured mesh generation, steady state solvers, and appropriate boundary conditions for airfoil case. Experimental procedures include wind tunnel testing at defined velocities and angles of attack.

2.1 Experimental Setup

The experimental setup involved a low-speed wind tunnel to measure aerodynamic forces on airfoil models as shown in table 1. The wind tunnel specifications included an open subsonic type with a flow speed range of 0–30 m/s. The lift calibration involved applying known weights on the airfoil model, with an average calibration factor of 1.43.

Table 1: Wind Tunnel Specifications

Specification	Details
Wind Tunnel Type	Open subsonic wind tunnel
Test Section Dimensions	Length: 1 m Width: 0.25 m Height: 0.25 m
Flow Speed Range	Minimum Velocity: 0 m/s Maximum Velocity: 30 m/s
Flow Measurement Equipment	Pitot-static tube for velocity measurements
Motor Specifications	Motor RPM: 2800
Airfoil Dimensions	Chord Length: 98mm Span: 150mm Thickness: 14.7mm
Environmental Conditions	Temperature: 300K

Instruments used for data acquisition included a Pitot-static tube for velocity measurements, a strain gauge for force measurement, and a two-component force balance to separate lift and drag forces. Velocity was calculated from manometric readings shown in table 2, with measurements ranging from 9.04 m/s to 15.66 m/s. These calibration data and instrument setups provided accurate and reliable measurements during the wind tunnel tests.

The velocity of airflow was measured using a Pitot-static tube, with readings from a manometer. The velocity was calculated using:

$$V = \sqrt{2g\Delta x \left(\frac{\rho_w}{\rho_a} - 1\right)} \tag{1}$$

where Δx is the manometer difference, ρw = 1000kg/m3, ρa = 1.2kg/m3, and g = 9.81m/s2.

Table 2: Manometer Readings and Velocity

RPM	x_1 (cm)	x_2 (cm)	Δx (cm)	V (m/s)
711	33.7	33.2	0.5	9.04
856	33.8	33.2	0.6	9.90
1002	33.9	33.1	0.8	11.43
1243	34.0	32.8	1.2	14.00
1411	34.1	32.6	1.5	15.66

2.2 Numerical Methodology

This study presents a comprehensive numerical investigation of the aerodynamic characteristics of a NACA 0015 airfoil using Computational Fluid Dynamics (CFD). The simulations were conducted in ANSYS Fluent with a steady-state, pressure-based solver, applying the standard k-epsilon turbulence model as given in table 3. Boundary conditions were applied with varying inlet velocities (9–15 m/s) and an angle of attack of 10° and 15° for the airfoil as illustrated in Table 3. In this study, angles of attack of 10° and 15° were chosen to analyze the aerodynamic performance of the NACA 0015 airfoil under both moderately attached and highly separated flow conditions. According to (Anderson , 2010) and (Abbott & Von Doenhoff, 1959), stall generally occurs near 15°, making these angles critical for understanding lift degradation and turbulence effects in post-stall regions. Previous CFD and experimental studies (Chakraborty & Mandal, 2020) also validate this selection for evaluating model accuracy and flow behavior across the stall boundary.

Table 3: Boundary Conditions for Airfoil CFD Simulation

Boundary Condition	Airfoil Simulation
Solver Type	Pressure-Based
Time	Steady state
Inlet Velocity	u =9–15 m/s
Operating Temperature	300 K
Outlet Pressure	Gauge Pressure = 0
Density of Fluid	ρ =1.2kg/m^3
Angle of Attack (AOA)	10° and 15°
Dynamic Viscosity	1.78×10^{-5} Pa · s
Number of Iterations	300
Initialization	Standard
Wall Condition	No-slip condition

Geometries were generated in ANSYS Design Modeler (Fig.s 4 and 5), with the airfoil profile imported from Airfoil Tools. The computational domain, as shown in Fig.s 4 and 5, was created in Design Modeler to define the spatial region for simulating fluid flow. This domain represents the physical space where governing equations like the Navier-Stokes equations are solved. A well-defined domain is essential for capturing accurate flow behavior and applying appropriate boundary conditions.

Fig. 4: Side View of Airfoil Domain with Dimensions.

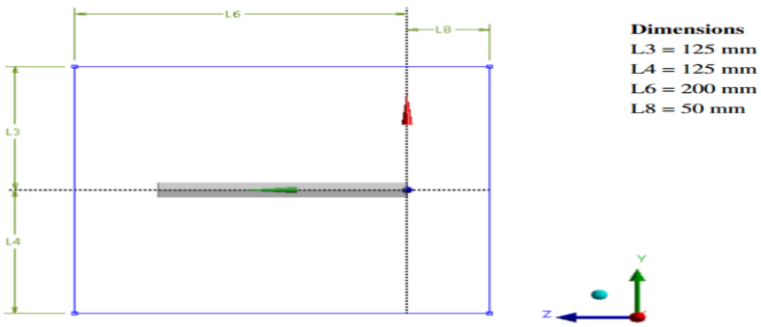

Fig. 5: Front View of Airfoil Domain with Dimensions.

A structured meshing approach with inflation layers was used to ensure accurate boundary layer resolution (Fig.s 6 and 7). Mesh quality significantly affects the accuracy and stability of CFD simulations. Poor grid quality can lead to convergence issues or unreliable results. To ensure accuracy, the mesh was refined iteratively following best practices (Pannirselvam, 2020). The computational domain was defined with appropriate boundary names—inlet, airfoil, and outlet—and designated as fluid. A smooth inflation layer with 10 layers and a growth rate of 1.2 was applied around the airfoil to capture boundary layer effects. Mesh settings included body sizing of 6mm, face sizing of 2mm, and

edge division of 200, as shown in Fig.s 6 and 7.

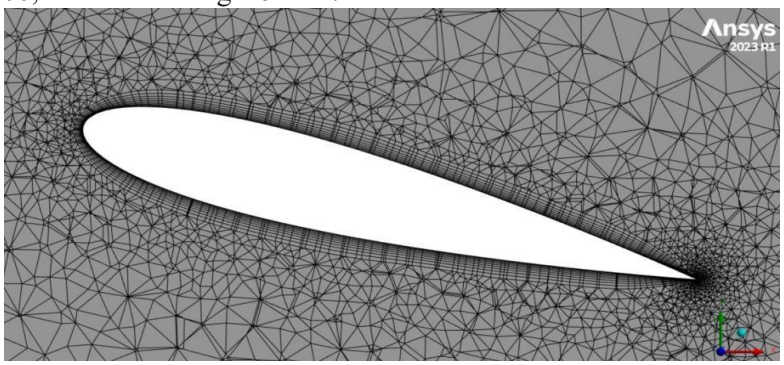

Fig. 6: Meshing around an airfoil.

Fig. 7: Meshing around domain.

The governing equations of fluid flow, including the continuity, momentum, and energy equations, were solved to predict aerodynamic forces. The study aims to analyze the impact of flow behavior on lift and drag forces and supports the design and optimization of aerodynamic components under subsonic conditions

The Mesh Independence Test ensures the accuracy and reliability of CFD results by identifying the mesh resolution beyond which further refinement has negligible impact on key outputs like lift and drag forces. Starting with a coarse mesh, simulations are repeated with increasingly finer meshes. When results converge and remain consistent across refinements, the solution is deemed mesh independent. This process balances computational efficiency with accuracy, validating that the simulation outcomes are not influenced by mesh size.

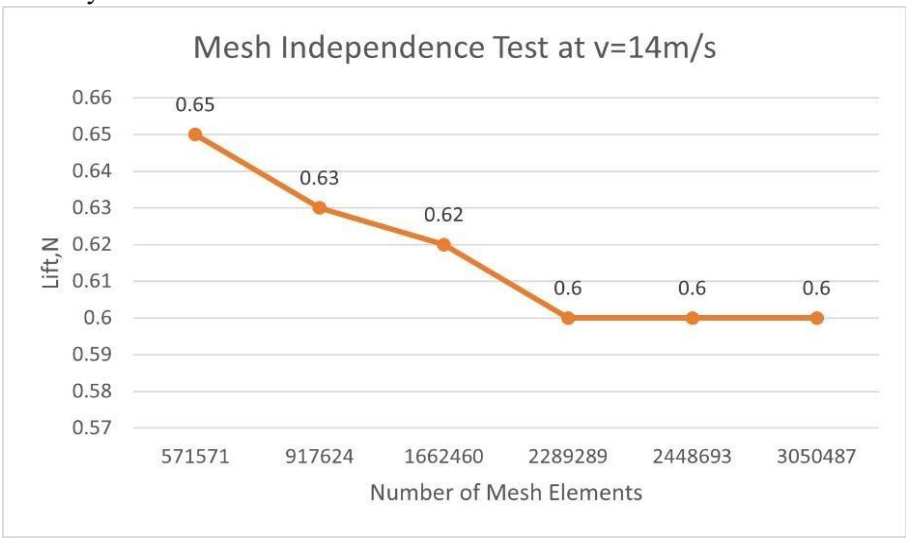

Fig. 8: Mesh Independence test of Airfoil at v=14 m/s.

3. Results and Discussion

The comparative analysis between experimental wind tunnel (WT) testing and computational fluid dynamics (CFD) simulations demonstrates a generally consistent trend in lift force behavior across varying flow velocities and angles of attack (AOA). Fig.s 9 and 10 present the lift force comparison for AOAs of 10° and 15°, respectively.

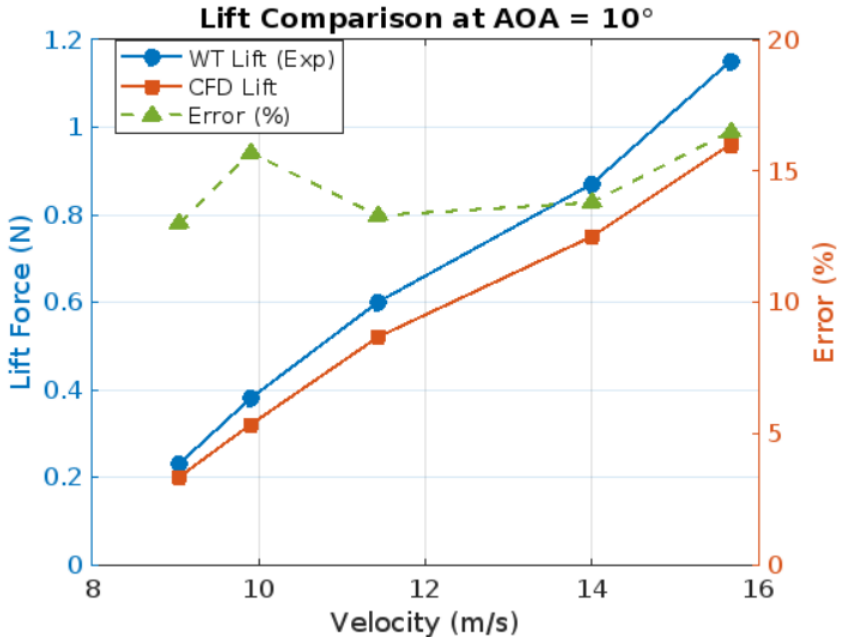

Fig. 9: Comparison of Lift Force in Airfoil at AOA=10°

The lift force at an angle of attack (AoA = 10°) and Reynolds number (Re= 74744) was measured from wind tunnel experiments, CFD simulations, and literature data. The wind tunnel experiment recorded a lift coefficient of 0.52, closely matching the literature value of 0.5122 with an error of 1.5% (Sheldahl and Klimas, 1981). However, the CFD simulation underpredicted the lift coefficient at 0.45, showing a 12% deviation. This discrepancy is likely due to turbulence model limitations, mesh resolution effects, and numerical discretization errors.

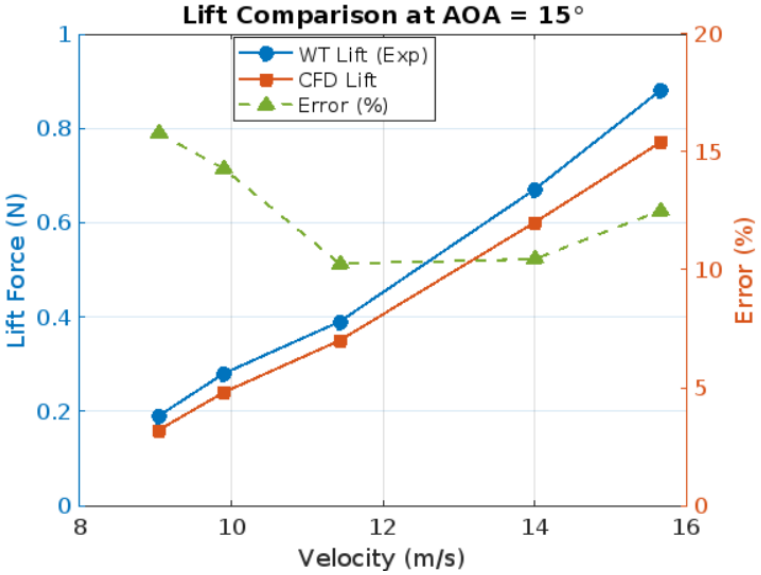

Fig. 10: Comparison of Lift Force in Airfoil at AOA=15°

At an angle of attack (AOA) of 15°, the lift coefficient (CL) for the NACA 0015 airfoil in this study was found to range from approximately 0.45 to 0.74 across velocities from 9.04 to 11.43 m/s, peaking at mid-range velocities before gradually declining at higher speeds. This behavior is indicative of the

onset of flow separation and stall, which aligns with the literature stating that stall typically initiates around 12°–15° for symmetric airfoils like NACA 0015 (Anderson, 2010; Abbott & Von Doenhoff, 1959). Reference data from (Abbott and Von Doenhoff , 1959) and (Chakraborty & Mandal, 2020) indicate that the expected CL for NACA 0015 at 15° AOA lies between 0.8 and 1.1 depending on the Reynolds number. Compared to this, the experimental values in the present study were lower by about 26% to 43%, suggesting possible early separation effects, wind tunnel blockage, or differences in Reynolds number and experimental setup.

Velocity and pressure contours from CFD simulations (Fig.s 11 and 12) revealed typical

aerodynamic behavior, such as high-velocity regions over the airfoil's upper surface. Fig. 11 presents the velocity distribution around the airfoil at an inlet velocity of 14m/s. A significant acceleration of airflow is observed over the airfoil's upper surface, represented by red and regions. This distribution aligns with Bernoulli's principle, highlighting the pressure drop over the upper surface that contributes to lift generation.

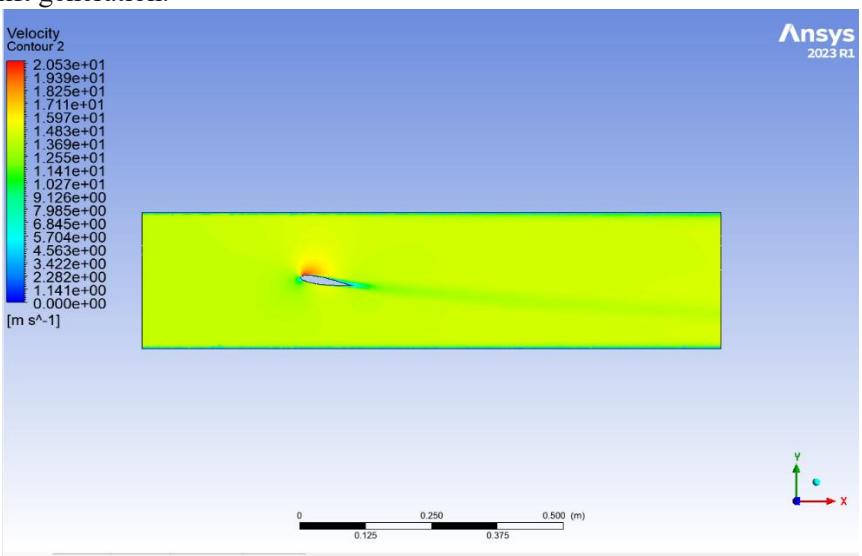

Fig. 11: Airfoil Velocity Contour

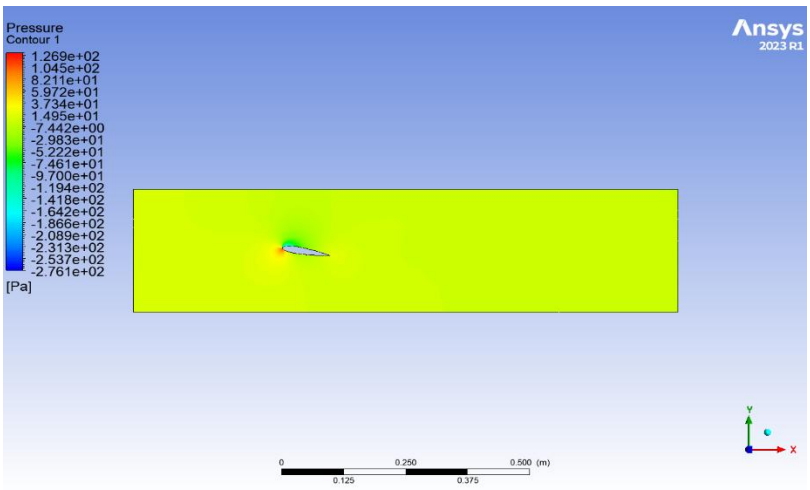

Fig. 12: Airfoil Pressure Contour

Fig. 12 illustrates the pressure distribution around the airfoil. High-pressure regions appear beneath the leading edge (red), while low pressure zones (blue/green) dominate the upper surface, consistent with Bernoulli's principle. This pressure differential, caused by accelerated airflow over the top surface, is the primary contributor to lift generation. Additionally, signs of flow separation and wake formation downstream of the airfoil can be observed particularly at higher AOAs. These phenomena are likely contributors to increased aerodynamic drag and reduced lift efficiency.

The CFD simulation provides a reasonably accurate estimation of lift forces and flow behavior

with errors falling within an acceptable range. Minor deviations highlight the importance of continued refinement in computational modeling and experimental calibration for improved fidelity in aerodynamic analysis.

4. Conclusion

The project successfully completed both experimental and CFD analysis of aerodynamic characteristics for NACA 0015 airfoil profile. The results obtained using the k-epsilon tur- bulence model in Ansys Fluent, showed good agreement with experimental data for lift force at angles of attack of 10° and 15°. This demonstrates the effectiveness of CFD as an alternative to experimental methods in aerodynamic studies. The findings offer valuable insights for enhancing aerodynamic performance in applications like aircraft wings and wind turbines. Future work could include transient state analysis, evaluation of different geometries, and a deeper investigation into pressure distribution over the airfoil.

Acknowledgement

This research was financially supported by the Research Management Cell (RMC) of Pashchimanchal Campus, Institute of Engineering, Tribhuvan University. The Authors are grateful for the funding assistance, which significantly contributed to the successful completion of this research

References

Aiman, N. N., & Samion, S. (2020). Evaluation of drag and lift forces of grooved cylinders in wind tunnel. Jurnal Mekanikal.

Anderson, J. (2011). Fundamentals of aerodynamics (SI units). McGraw-Hill.

Arabacı, S., & Kiraz, E. (2023). A new force measurement mechanism in wind tunnel: CFD and experimental validation on a cylinder. Journal of Scientific Reports-A, (053), 16–27.

Kütahya Dumlupınar University.

Barlow, J. B., Rae, W. H., & Pope, A. (1999). Low-speed wind tunnel testing. John Wiley & Sons.

Boyle, M. T. (1988). Low speed wind tunnel testing. In Fourth annual IEEE semiconductor thermal and temperature measurement symposium (pp. 31–39). IEEE.

Burdett, T., Gregg, J., & Van Treuren, K. (2011). An examination of the effect of Reynolds number on airfoil performance. In Energy Sustainability (Vol. 54686, pp. 2203–2213).

Chakraborty, N. (2021, May). Turbulence modelling of air flow around an aerofoil. https://doi.org/10.13140/RG.2.2.25981.49125

Dash, A. (2016). CFD analysis of wind turbine airfoil at various angles of attack. IOSR Journal of Mechanical and Civil Engineering, 13(4), 18–24.

Dean, B., & Bhushan, B. (2010). Shark-skin surfaces for fluid-drag reduction in turbulent flow: A review. Philosophical Transactions of the Royal Society A: Mathematical, Physical and Engineering Sciences, 368(1929), 4775–4806.

Dreesecode.(2025).Airfoilprimer.

https://www.dreesecode.com/primer/BACKUPS_PUBLISH_JAN_17/airfoil2.ht

ml (Accessed: February 27, 2025)

Elsheltat, S. F., Alshara, A. A., Altaweel, A. A., & Abdulsalam, E. (2024). Numerical investigation of NACA-0015 airfoil performance using ANSYS: A detailed study of lift, drag, and stall characteristics. 15–01 ,(2)28 ,ꝛz.

FeaTips. (2021). Mesh quality and advanced topics. https://featips.com/wpcontent/uploads/2021/05/Mesh-

Intro_16.0_L07_Mesh_Quality_and_Advanced_Topics.pdf (Accessed: March 4, 2025)

İzzet, Ş., & Acir, A. (2015, February). Numerical and experimental investigations of lift and drag performances of NACA 0015 wind turbine airfoil. International Journal of Materials, Mechanics and Manufacturing.

Layton, W. J., & Lewandowski, R. (2002). Analysis of an eddy viscosity model for large eddy simulation of turbulent flows. Journal of Mathematical Fluid Mechanics, 4(4), 374–399.

Liu, X., Levitan, M., & Nikitopoulos, D. (2008). Wind tunnel tests for mean drag and lift coefficients on multiple circular cylinders arranged in-line. Journal of Wind Engineering and Industrial Aerodynamics, 96(6–7), 831–839.

Mallick, M. (2016). Study on drag coefficient for the flow past a cylinder. ResearchGate. https://www.researchgate.net/publication/303459692_Study_on_Drag_Coefficient_for_the_Flow_Past_a_Cylinder

Mathieu, J., & Scott, J. (2000). An introduction to turbulent flow. Cambridge University Press.

Miller, S. D. (2008). Lift, drag and moment of a NACA 0015 airfoil. Department of Aerospace Engineering, 28.

Paraschivoiu, I. (2003). Subsonic aerodynamics. Presses inter Polytechnique.

Pannirselvam, M. (2020). Simulation of airfoil flow and determination of induced drag with Ansys-Fluent (Master's thesis, Hamburg University of Applied Sciences).

RNG. (2012). RNG k-Epsilon model. https://www.scribd.com/document/99021532/Chp12-RNG-K-Epsilon (Accessed:

March 3, 2025)

Rubel, R. I., Uddin, M. K., Islam, M. Z., & Rokunuzzaman, M. D. (2016). Numerical and experimental investigation of aerodynamics characteristics of NACA 0015 aerofoil. International Journal of Engineering Technologies (IJET), 2(4), 132–141.

Salleh, S. (2004). Development and improvement of subsonic wind tunnel in Universiti Teknologi Petronas (air flow quality testing). Universiti Teknologi Petronas.

Sheldahl, R. E., & Klimas, P. C. (1981). Aerodynamic characteristics of seven symmetrical airfoil sections through 180-degree angle of attack for use in aerodynamic analysis of vertical axis wind turbines. Sandia National Laboratories.

Suchdev, A. (2020). Airfoil design and lift (Part 2).

Uddin, M. K., Islam, M. Z., Rokunuzzaman, M., & Rubel, R. I. (2015). Experimental and numerical measurement of lift and drag force of NACA 0015 airfoil blade. In International Conference on Mechanical, Industrial and Materials Engineering 2015.

Verma, N., & Baloni, B. D. (2019). Numerical and experimental investigation of flow in an open-type subsonic wind tunnel. SN Applied Sciences, 1(11), 1384.

Yılmaz, M., Köten, H., Çetinkaya, E., & Coşar, Z. (2018). A comparative CFD analysis of NACA0012 and NACA4412 airfoils. Journal of Energy Systems, 2(4), 145–159.

Airfoil Tools. (2025). NACA 4-digit airfoil generator. http://airfoiltools.com/airfoil/naca4digit (Accessed: March 4, 2025)

Anderson, J. D. (2010). Fundamentals of aerodynamics (5th ed.). McGraw-Hill.

Abbott, I. H., & Von Doenhoff, A. E. (1959). Theory of wing sections. Dover Publications.

Menter, F. R. (1994). Two-equation eddy-viscosity turbulence models for engineering applications. AIAA Journal, 32(8), 1598–1605. https://doi.org/10.2514/3.12149

Chakraborty, A., & Mandal, B. (2020). Materials Today: Proceedings, 26, 2242–2247.https://doi.org/10.1016/j.matpr.2020.02.459